eLIFE elifesciences.org

RESEARCH ARTICLE

Figures and figure supplements

Phosphoproteomics reveals that Parkinson's disease kinase LRRK2 regulates a subset of Rab GTPases

Martin Steger *et al*

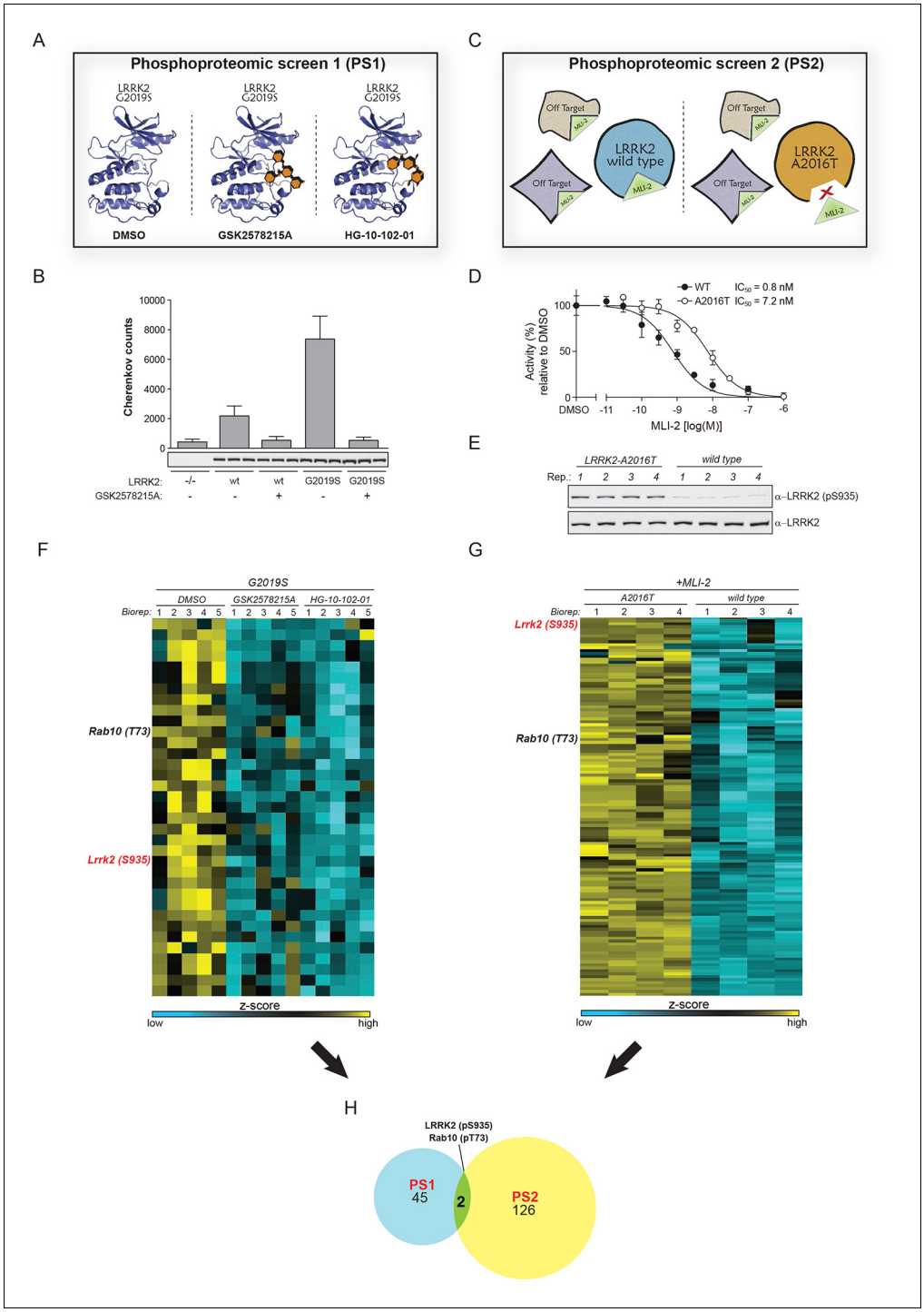

Figure 1. Two unbiased phosphoproteomic screens identify physiological LRRK2 targets. (**A**) Experimental setup of PS1. LRRK2-G2019S^{GSK} mouse embryonic fibroblasts (MEFs, n=5) were treated with DMSO or each of two structurally distinct LRRK2 inhibitors GSK2578215A or HG-10-102-01 (1 μM for 90 min). (**B**) LRRK2 immunoprecipitated from either knockout (-/-), wild-type (wt) or LRRK2-G2019S^{GSK} (G2019S) knock-in MEFs was assessed for phosphorylation of Nictide (***Nichols et al., 2009***) peptide substrate in absence or presence of GSK2578215A (2 μM). Western blot below shows that similar levels of LRRK2 were immunoprecipitated. Error bars are mean ± SD (n=3). (**C**) Scheme of PS2. The higher affinity of MLI-2 toward wt-LRRK2 allows specific pinpointing of LRRK2 substrates when comparing the phosphoproteomes of wt and A2016T MEFs. (**D**) Kinase activities of wt (closed circles) and A2016T (open circles) GST-LRRK2 [1326-2527] purified from HEK293 cells were assayed in the

Figure 1 continued on next page

Figure 1 continued

presence of the indicated concentration of MLI-2 (n=3). (**E**) Decreased levels of pS935-LRRK2 in wt MEFs after treatment with 10 nM MLI-2. (**F**) Heat map cluster of phosphopeptides in PS1 ($p<0.005$) which are downregulated after treatment with both GSK2578215A and HG-10-102-01. (**G**) Heat map cluster of downregulated (FDR=0.01, S0=0.2) phosphopeptides in PS2. (**H**) Venn diagram of overlapping downregulated phosphosites in PS1 and PS2. (Biorep= biological replicate). SD, standard deviation.

DOI: 10.7554/eLife.12813.003

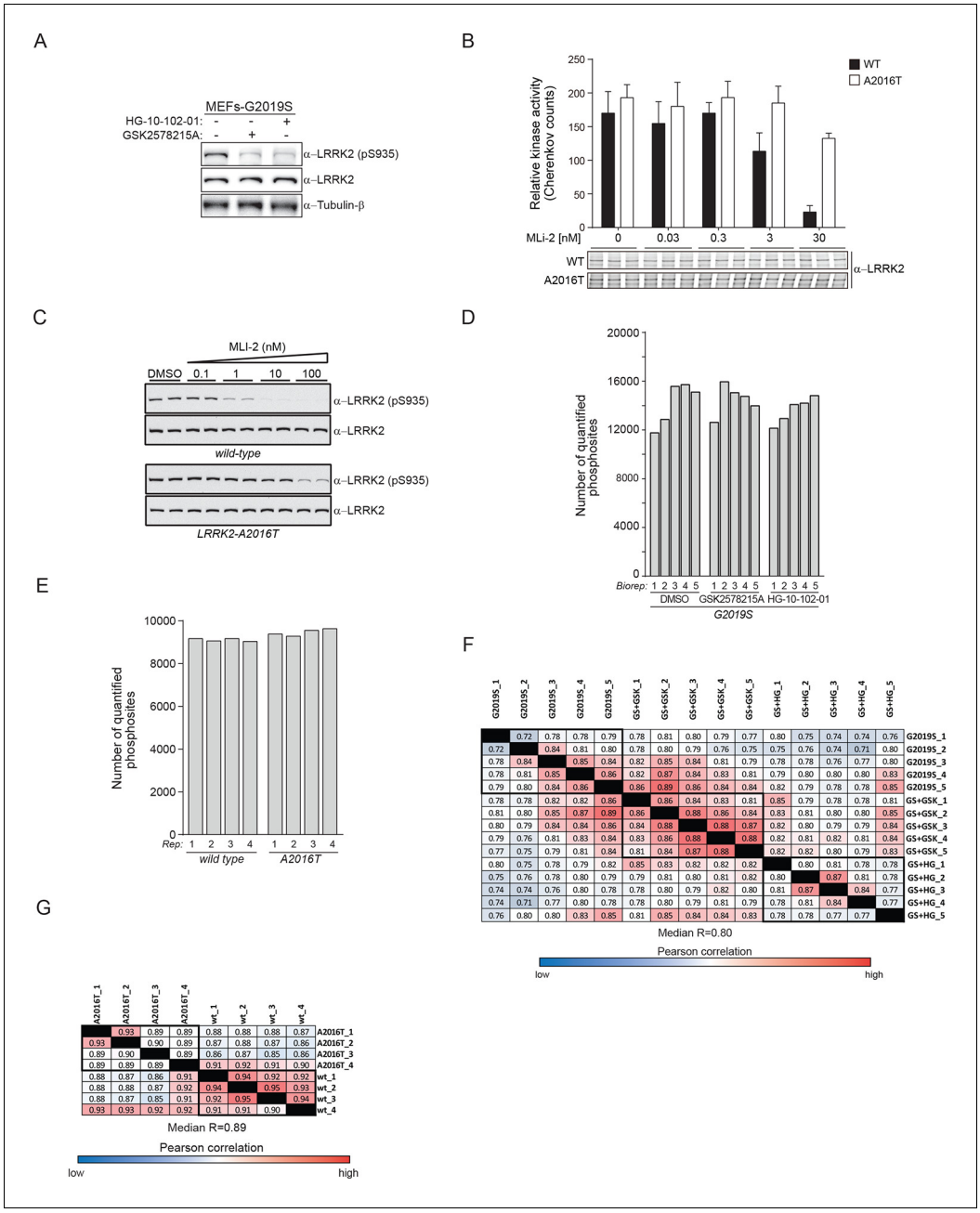

Figure 1—figure supplement 1. Two unbiased phosphoproteomic screens identify physiological LRRK2 targets. (**A**) Western blot analysis of wild type (wt) and LRRK2-G2019S^{GSK} (G2019S) mouse embryonic fibroblasts (MEFs), treated with DMSO (-) or 1 μM of GSK2578215A or HG-10-102-01 for 90 min. (**B**) In vitro kinase assay using LRRK2 immunoprecipitated from MEFs (wt and A2016T) in the presence of various concentrations of MLi-2. Phosphorylation of Nictide was quantified by liquid scintillation counting. The western blot below shows that similar levels of LRRK2 were used. Error bars are mean ± SD (n=3). (**C**) Western blot analysis of pS935-LRRK2 and total LRRK2 levels in wt-LRRK2 MEFs and A2016T-LRRK2 MEFs treated for 60 min with the indicated concentrations of MLI-2. (**D**) Number of quantified class I phosphorylation sites of PS1 in five biological replicates (Biorep) per phenotype analyzed. (**E**) More than 9000 phosphorylation sites are identified in each of the four biological replicates (Biorep) of wild type and A2016T MEFs (PS2). (**F**) Pearson correlations for the phosphoproteomes of PS1 and PS2 (**G**). SD, standard deviation.

DOI: 10.7554/eLife.12813.004

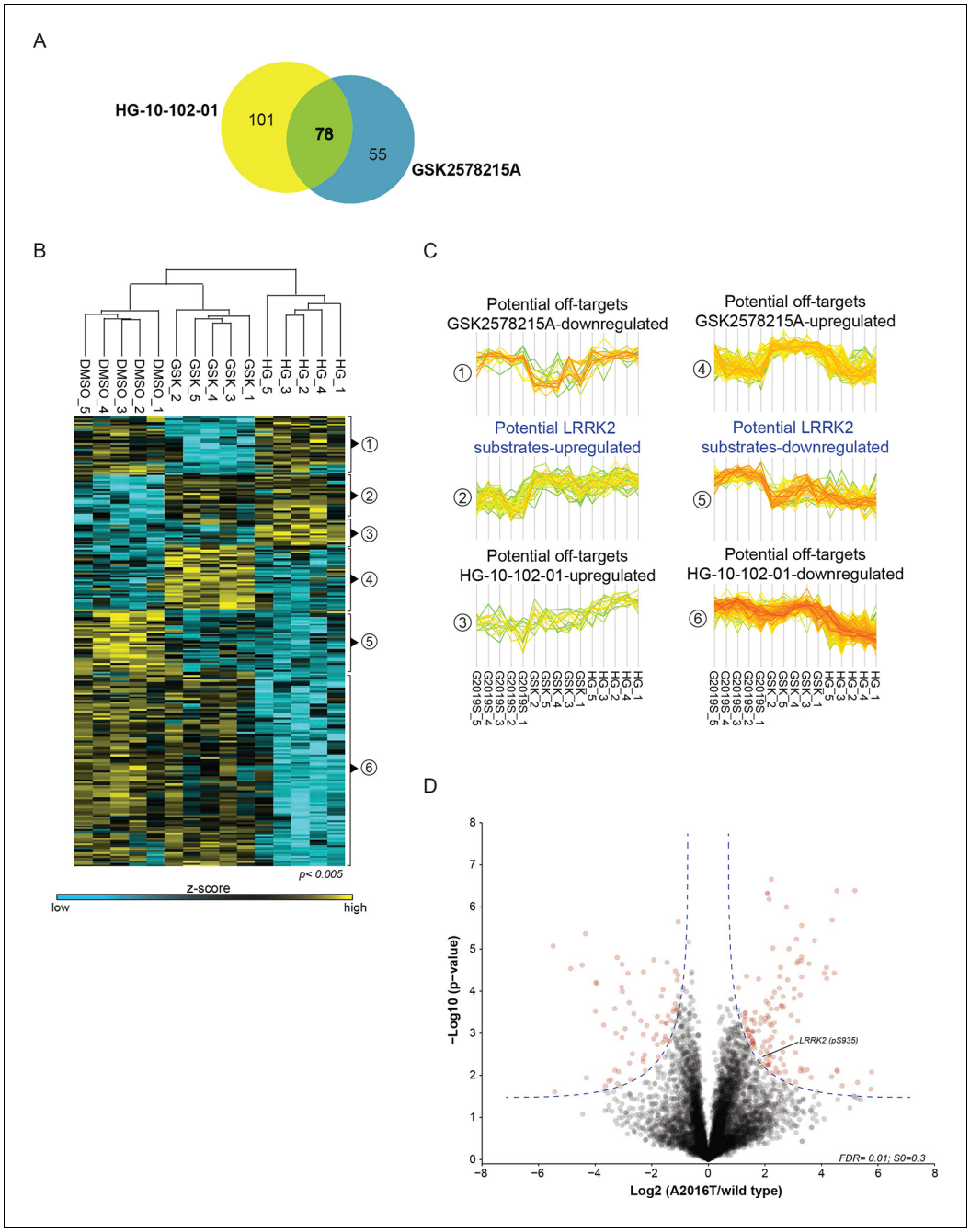

Figure 1—figure supplement 2. Two unbiased phosphoproteomic screens identify physiological LRRK2 targets. (**A**) Venn diagram of significantly regulated (ANOVA, p<0.005) sites with GSK2578215A and HG-10-102-01 in PS1. (**B**) Heat map of regulated phosphosites identified in five biological replicates of MEFs (LRRK2-G2019S^{GSK} (DMSO), LRRK2-G2019S^{GSK}+ GSK2578215A. and LRRK2-G2019S^{GSK} + HG-10-102-01). (**C**) Clusters identified in (**B**). (**D**) Volcano plot of all phosphosites of PS2. Significant sites are in blue and pS935 is indicated. ANOVA, analysis of variance.

DOI: 10.7554/eLife.12813.005

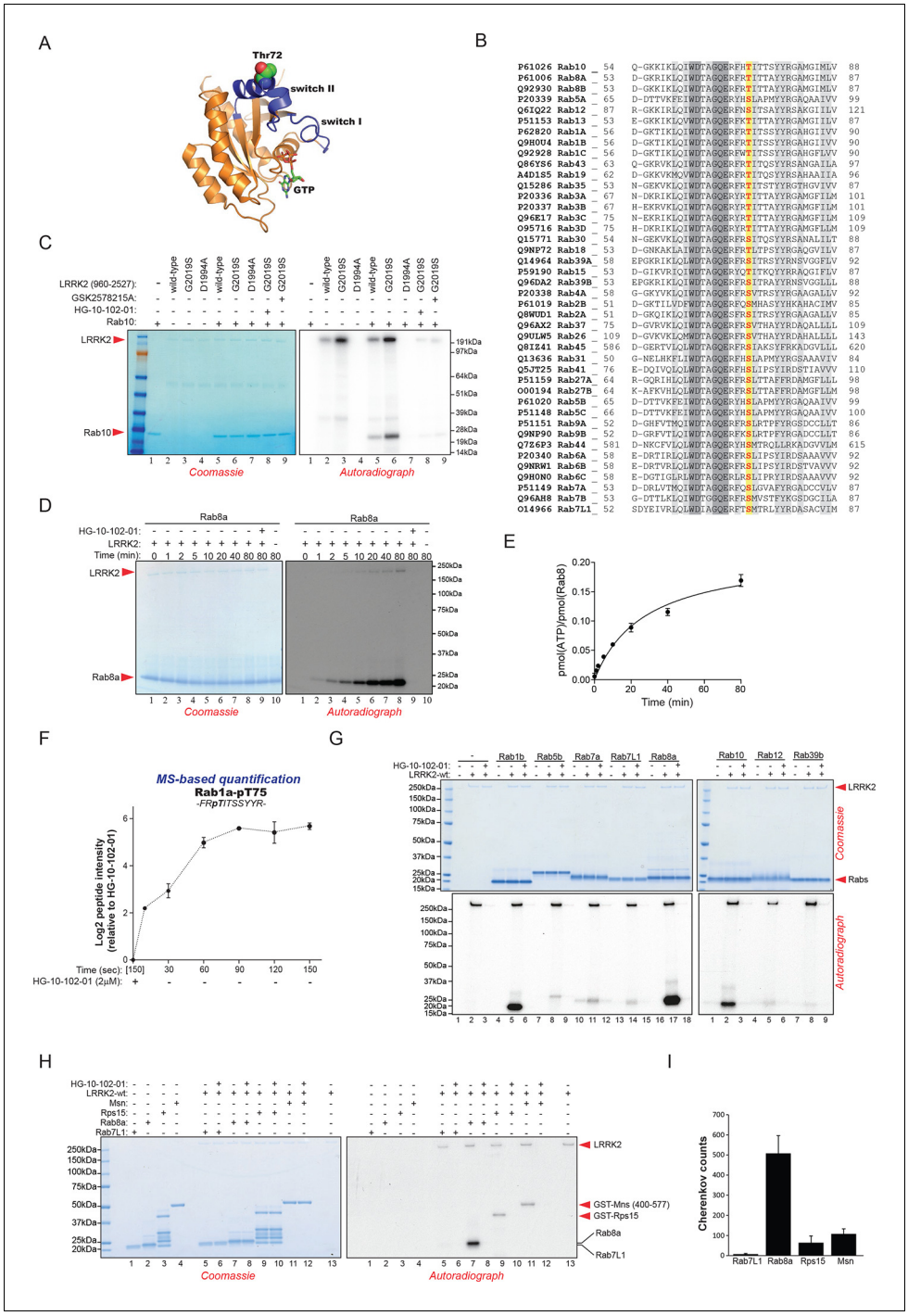

Figure 2. Phosphorylation of Rab GTPases by LRRK2 in vitro. (**A**) Position of threonine 72 in the switch II region of Rab8a (PDB: 4HLY). (**B**) Sequence alignment of Rab10 and other indicated Rab-family members. (**C**) Phosphorylation of Rab10 (1 µM) by wt-, G2019S- or kinase inactive LRRK2-D1994A. Inhibition of LRRK2-G2019S by GSK2578215A or HG-10-102-01 prevents phosphorylation. (**D**) Time course of LRRK2 (wt) mediated Rab8a (4 µM) phosphorylation and (**E**) quantification of phosphorylation stoichiometry (n=3). (**F**) Time course of LRRK2-wt-mediated pT75-Rab1a phosphorylation and MS-based label-free quantification (n=3). (**G**) In vitro phosphorylation of recombinant Rab proteins (4 µM) by LRRK2-wt. (**H**) Phosphorylation of recombinant Rab7L1, Rab8a, moesin, and Rps15 by LRRK2 and (**I**) quantification of the signals. For all reactions LRRK2 inhibitors= 2 µM and LRRK2= 100 ng. Error bars indicate mean ± SEM of replicates. MS, mass spectrometry; SEM, standard error of the mean; wt, wild type.

DOI: 10.7554/eLife.12813.006

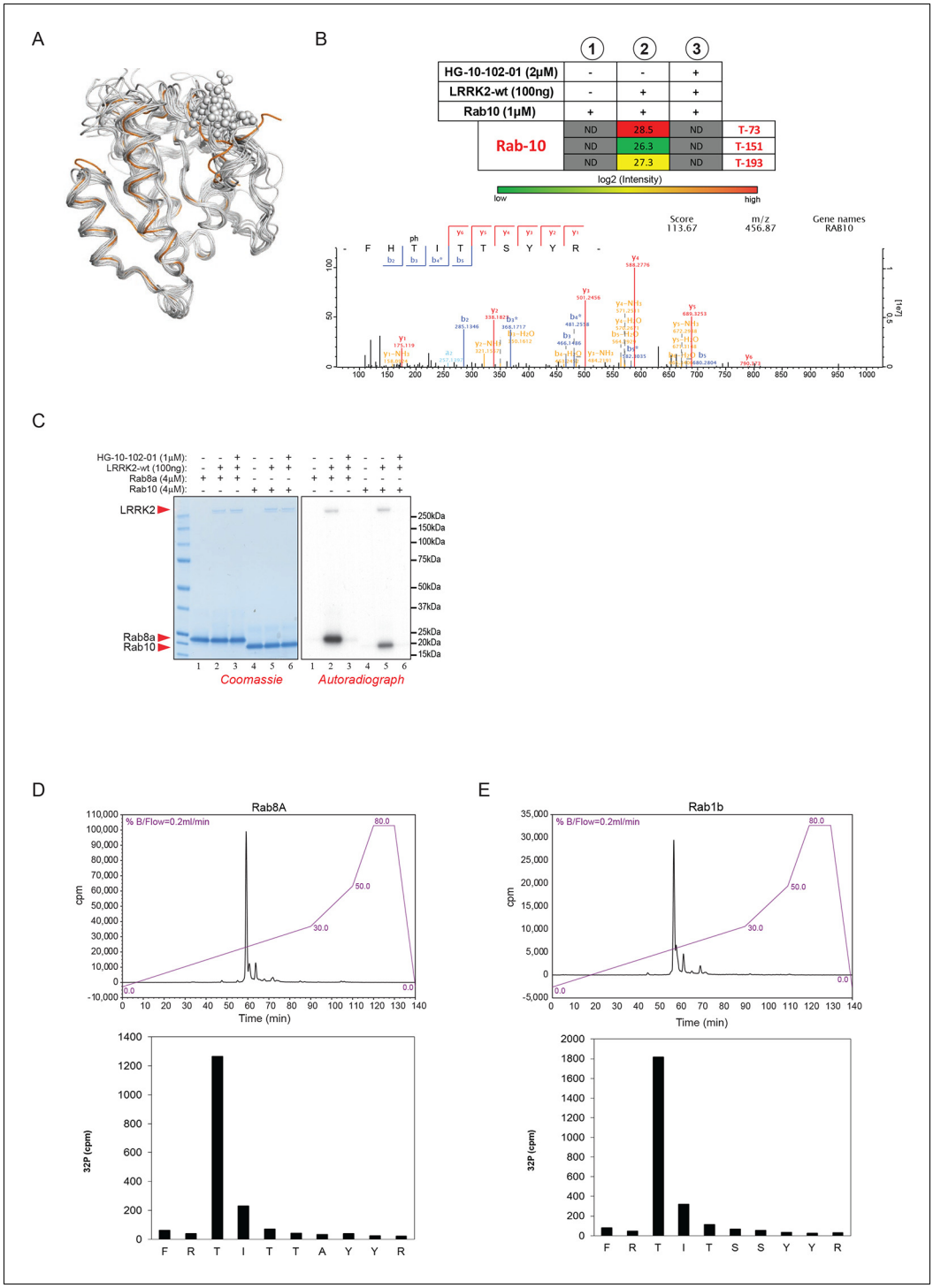

Figure 2—figure supplement 1. Phosphorylation of Rab GTPases by LRRK2 in vitro. (**A**) Superposition of the crystal structures of 14 Rab isoforms (Rab1a, 1b, 2, 3, 4, 6, 7, 9, 12, 18, 27, 30, 31, 43). All potential LRRK2 phosphorylation sites (in grey) cluster in the same region. (**B**) MS analysis of in vitro phosphorylated Rab10 identified three LRRK2-specific sites (note that phosphorylation is prevented completely by HG-10-102-01) and pT73 as the one with the highest intensity. The collision-induced dissociation (CID) fragmentation spectrum and the Andromeda score (score) (***Cox et al., 2011***) for the tryptic pT73-Rab10 peptide are shown. (**C**) Phosphorylation of Rab8a and Rab1b by LRRK2-wt. Inhibition of LRRK2 by HG-10-102-01 prevents phosphorylation. (**D**) HPLC trace of tryptic peptides of Rab8a and Rab1b (**E**) after in vitro phosphorylation by LRRK2-wt and

Figure 2—figure supplement 1 continued on next page

Figure 2—figure supplement 1 continued

sequence analysis of tryptic peptides. Y axis units are relative Cherenkov counts per minute. MS, mass spectrometry; wt, wild type.

DOI: 10.7554/eLife.12813.007

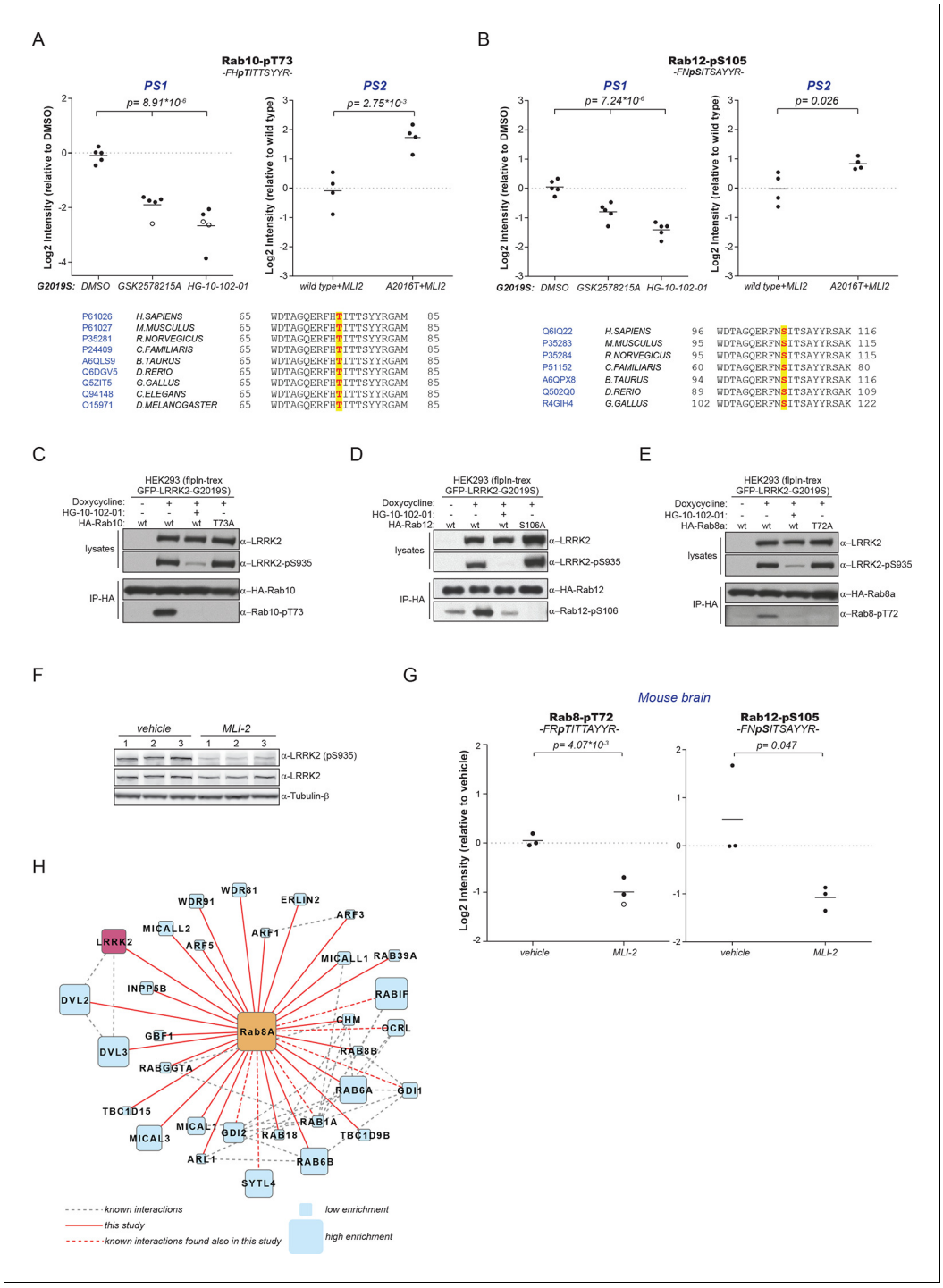

Figure 3. A number of Rab GTPases are physiological LRRK2 substrates. (**A**) MS-quantified pT73-Rab10 peptide intensities in PS1 and PS2. Sequence alignment of the T73-Rab10 region is shown below. (**B**) Same as (**A**) with pS106-Rab12. Western blots illustrating phosphorylation of T73-HA-Rab10 (**C**), S106-HA-Rab12 (**D**), and T72-Rab8 (**E**) after induction of LRRK2 expression by doxycycline (1 µg/ml). HG-10-102-01 (1 µM) was added prior to lysis. (**F**) Western blot of homogenized brain lysates from LRRK2-G2019S^{Lilly} mice injected with vehicle (40% HPβCD) or with 3 mg/kg MLI-2 (Biorep= biological replicate) and (**G**) MS-based quantification of pT72-Rab8 and pS105-Rab12 peptides. (**H**) Cytoscape network analysis of Rab8a interacting proteins determined by affinity-purification mass spectrometry (AP-MS). LRRK2 is in purple and dashed lines in grey show experimentally determined interactions from string database (http://string-db.org/).

DOI: 10.7554/eLife.12813.008

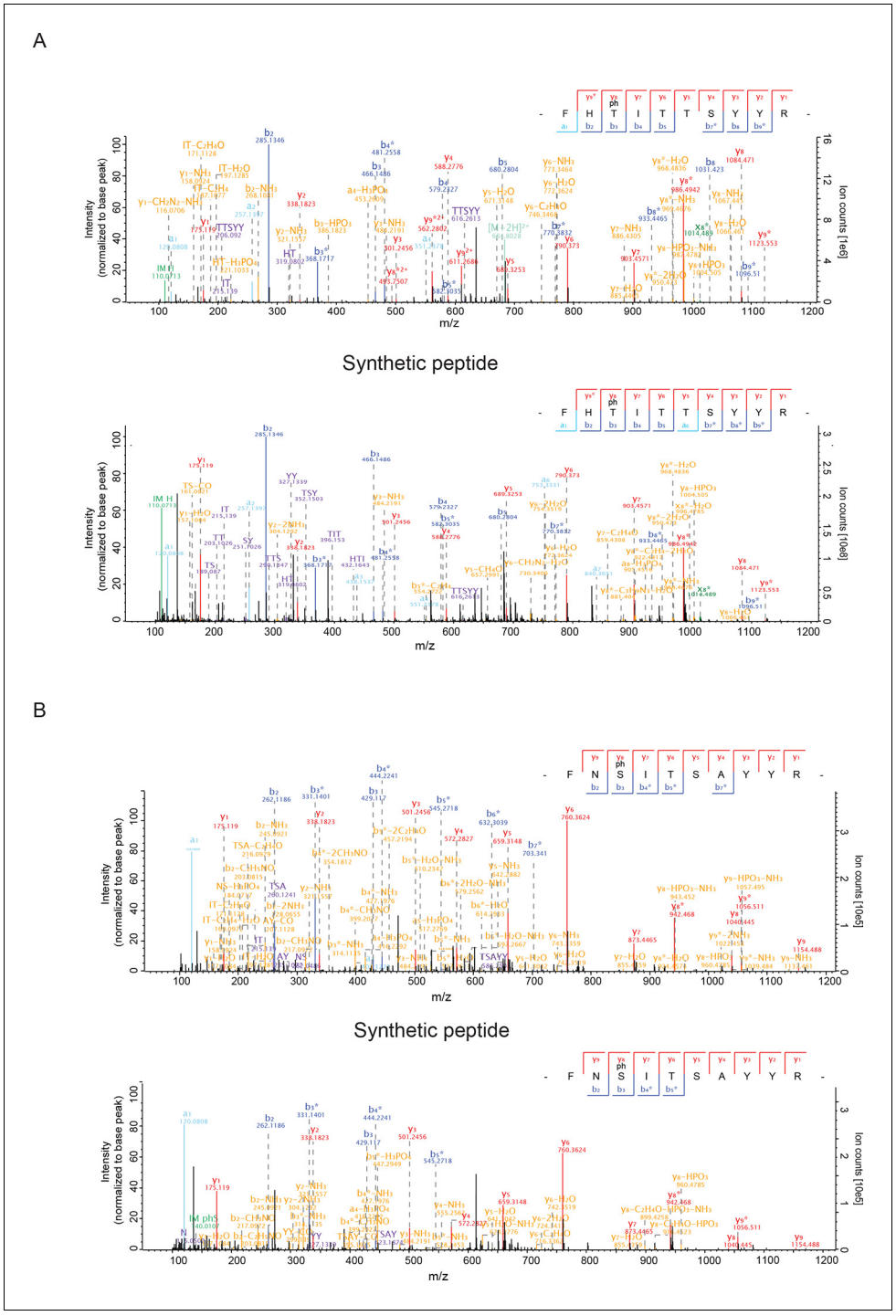

Figure 3—figure supplement 1. HCD MS/MS spectra of synthetic Rab peptides (**A**) Higher energy collision-induced dissociation (HCD) MS/MS spectra of the pT73-Rab10 peptide identified in PS2. The spectrum of the corresponding synthetic peptide is shown below. (**B**) Same as (**A**) but pS105-Rab12.

DOI: 10.7554/eLife.12813.009

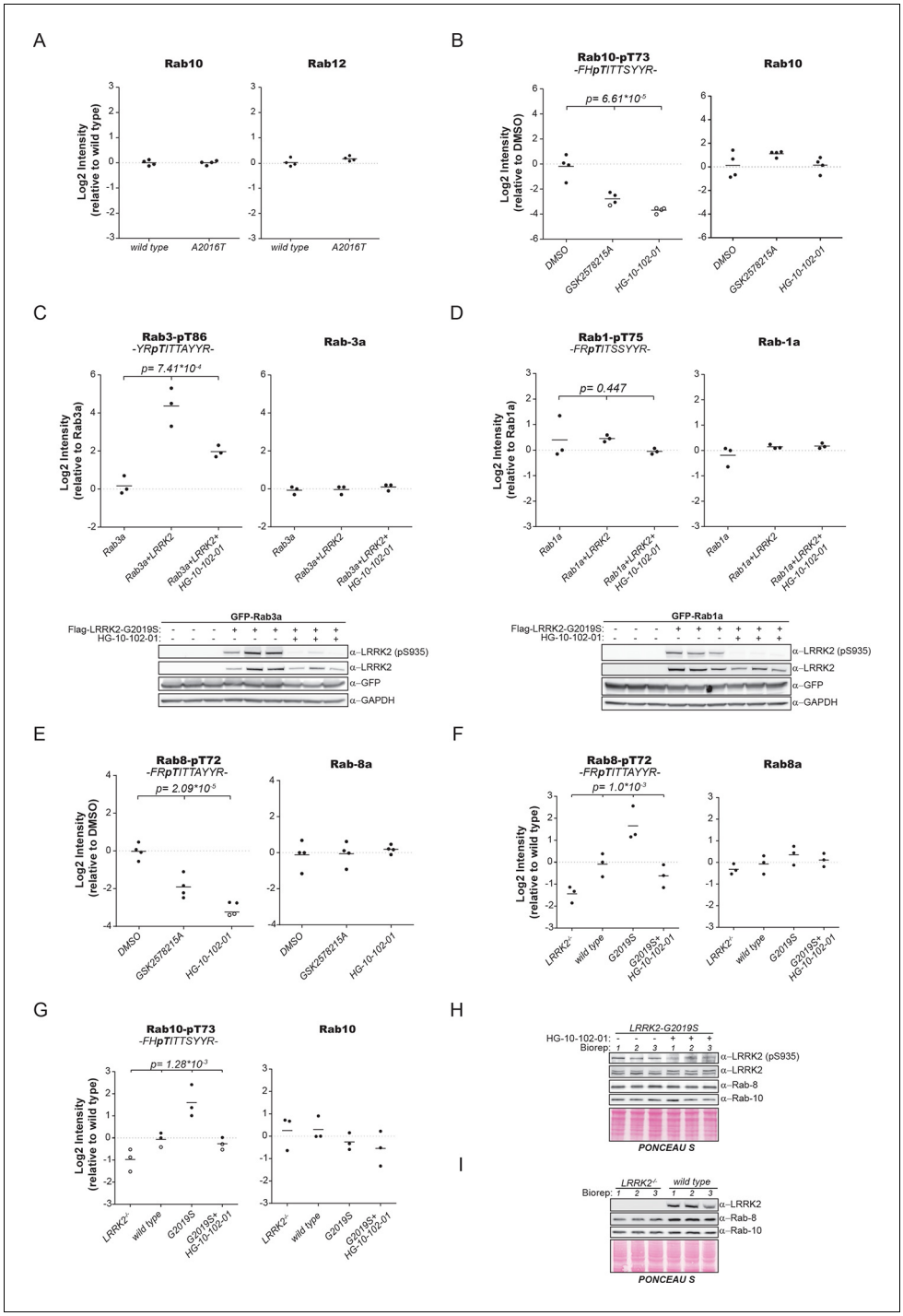

Figure 3—figure supplement 2. Quantification of Rab phosphorylation by mass spectrometry (MS). (**A**) MS-based label-free quantification (MaxLFQ, ***Cox et al., 2014***) of the Rab10 and Rab12 protein intensities in PS2. (**B**) MS-based quantification of pT73-Rab10 (left) and total Rab10 (right) derived from HEK293 (trex flpIn) cells expressing GFP-LRRK2-G2019S after LRRK2 inhibition (n=4). (**C**) MS-quantified Rab3-pT86 peptide levels of ectopically expressed Rab3a alone or in combination with LRRK2-G2019S, in presence or absence of HG-10-102-01 (3 μM, 3 hr, n=3). A western blot of the same samples is shown below. (**D**) Same as (**C**) but Rab1a was expressed and pT75-Rab1a quantified. (**E**) Same as (**B**) with pT72-Rab8 (left) and total Rab8a (right). (**F**) Label-free quantification of pT73-Rab10 and (**G**) pT72-Rab8a from knockout, wt, G2019S, or G2019S treated with HG-10-102-01 (3 μM, 3 hr) MEFs. Total Rab10 and Rab8 protein levels were also quantified (n=3). (**H**) and (**I**) Western blot analyses of samples used in (**F**) and (**G**). Open circles indicate imputed values. MEFs, mouse embryonic fibroblasts; wt, wild type.
DOI: 10.7554/eLife.12813.010

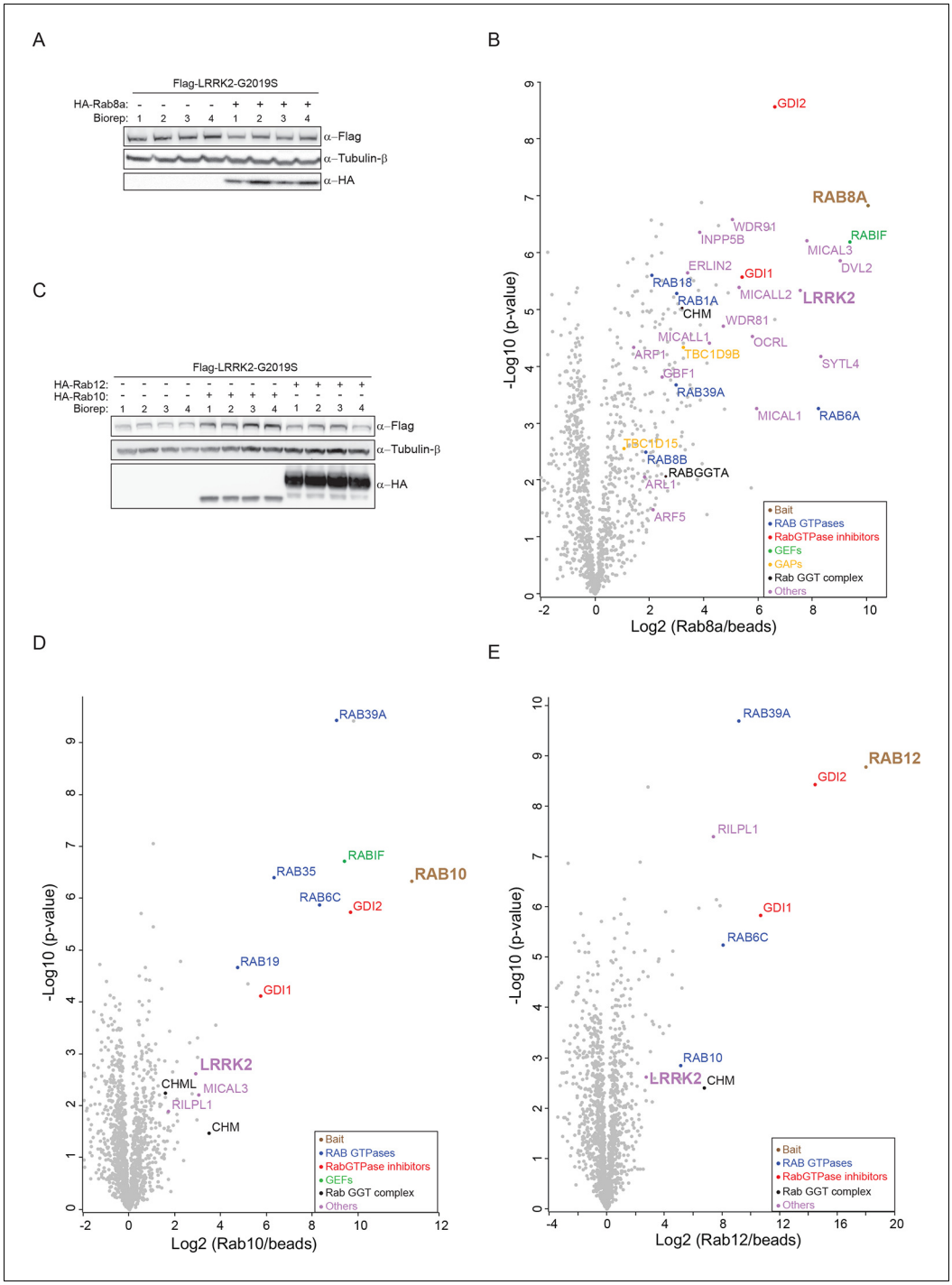

Figure 3—figure supplement 3. Several Rabs stably associate with LRRK2 in cells. (**A**) Western blot of HEK293 cells expressing flag-LRRK2-G2019S, either alone or in combination with HA-Rab8a. (**B**) Volcano plot of MS-quantified Rab8a interactors (n=4). (**C**) Same as (**A**) with HA-Rab10 or HA-Rab12. (**D**) and (**E**) Volcano plots of MS-quantified Rab10 and Rab12 interactors. MS, mass spectrometry.

DOI: 10.7554/eLife.12813.011

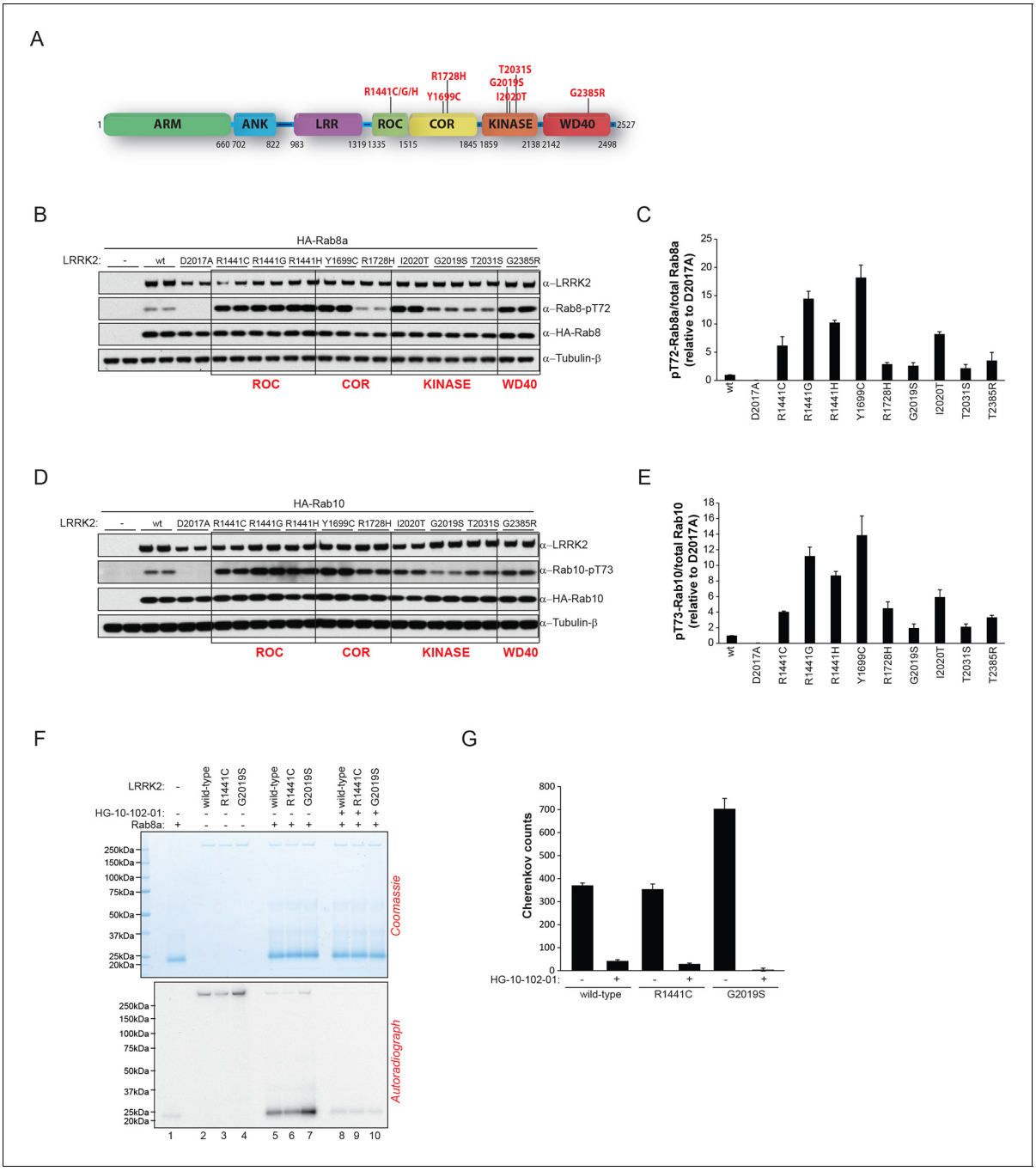

Figure 4. LRRK2 pathogenic variants increase phosphorylation of Rab GTPases. (**A**) Scheme of LRRK2 and common PD-associated amino acid substitutions (in red). (**B**) Different LRRK2 versions were co-expressed with Rab8a in HEK293 cells, lysates subjected to immunoblot analysis and (**C**) indicated signals quantified. (**D**) and (**E**) Same as (**B**) but HA-Rab10 was used. (**F**) In vitro phosphorylation of recombinant Rab8a (4 µM) by indicated LRRK2 variants (100 ng) and (**G**) quantification of the signals. HG-10-102-01= 2 µM. Error bars indicate mean ± SEM of replicates (n=3). PD, Parkinson's disease; SEM, standard error of the mean.

DOI: 10.7554/eLife.12813.012

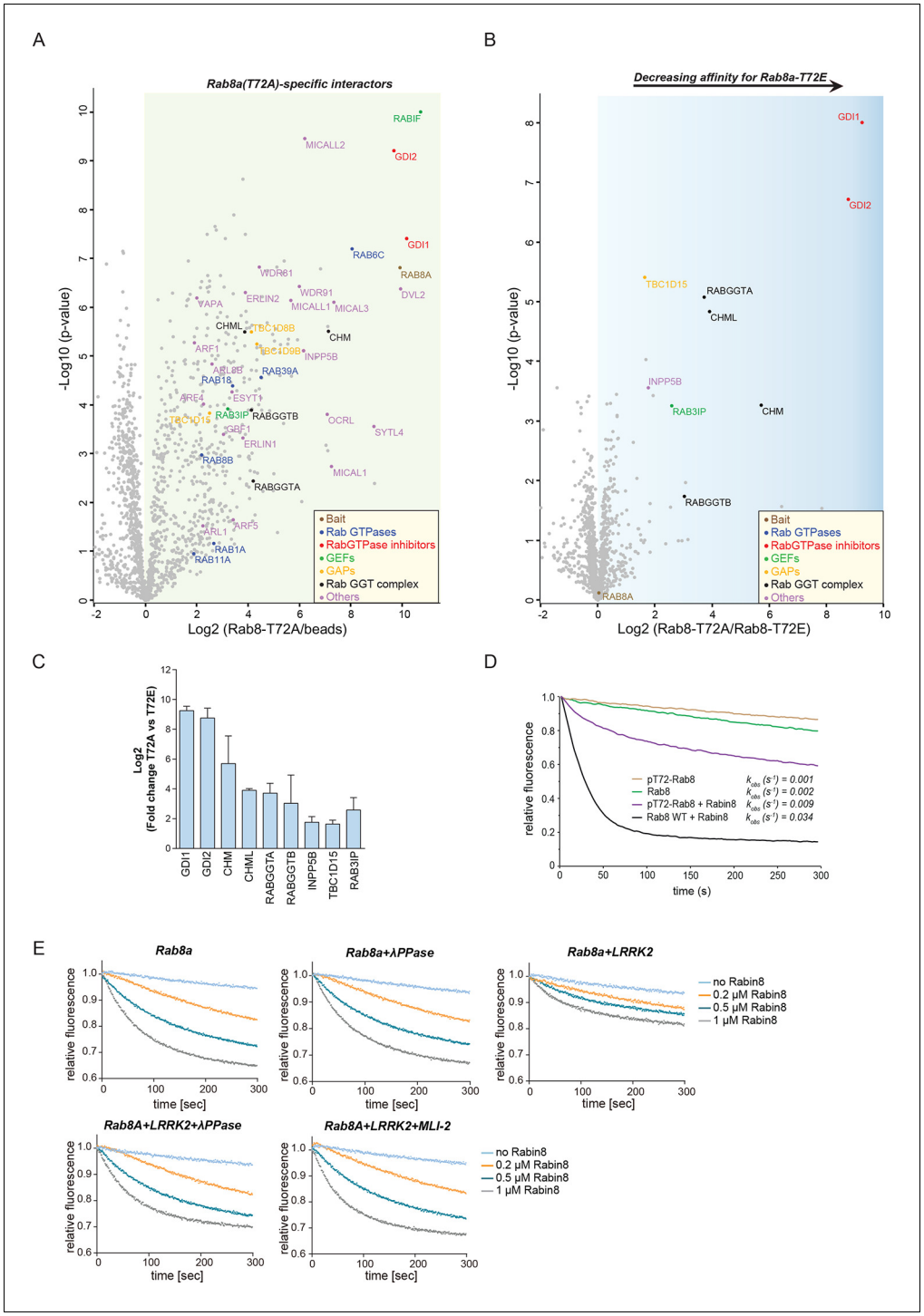

Figure 5. LRRK2 controls the interaction of Rabs with regulatory proteins. (**A**) Volcano plots showing interactors of GFP-Rab8a (T72A) transiently expressed in HEK293 cells and (**B**) Proteins differentially binding to T72A as compared to T72E. (**C**) Fold changes (T72A/T72E, n=4) of regulated proteins shown in (**B**). (**D**) Kinetic measurements of the dissociation of mant-GDP from non-phosphorylated and T72 phosphorylated Rab8a by Rabin8. Observed rate constants (k_{obs}) are indicated for each reaction and data points represent mean (n=3). (**E**) Measurements of mant-GDP dissociation from LRRK2 phosphorylated Rab8a by Rabin8 in absence or presence of λ-phosphatase (λ-PPase) or MLI-2 (1 μM). Error bars are mean ± SD of replicates.

DOI: 10.7554/eLife.12813.013

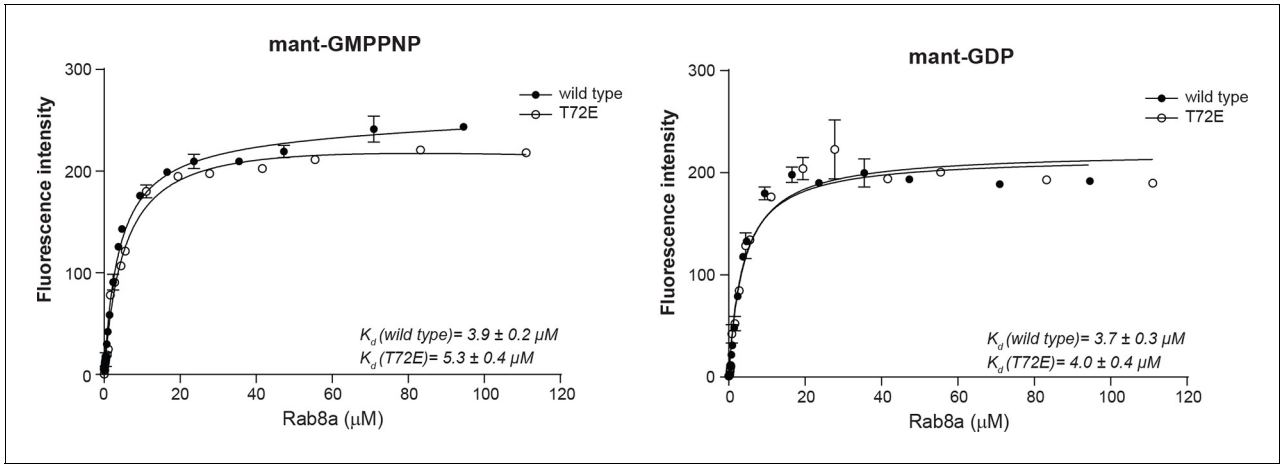

Figure 5—figure supplement 1. Rab8a nucleotide binding experiments. Titration experiment using Rab8a (wt and T72E) and fluorescently labeled non-hydrolysable GTP analog (mant-GMPPNP) or GDP (mant-GDP). The fluorescence signal is plotted as a function of Rab8a concentration. The dissociation constants (K_d) ± SD are indicated. Error bars are mean ± SD (n=3). SD, standard deviation; wt, wild type.
DOI: 10.7554/eLife.12813.014

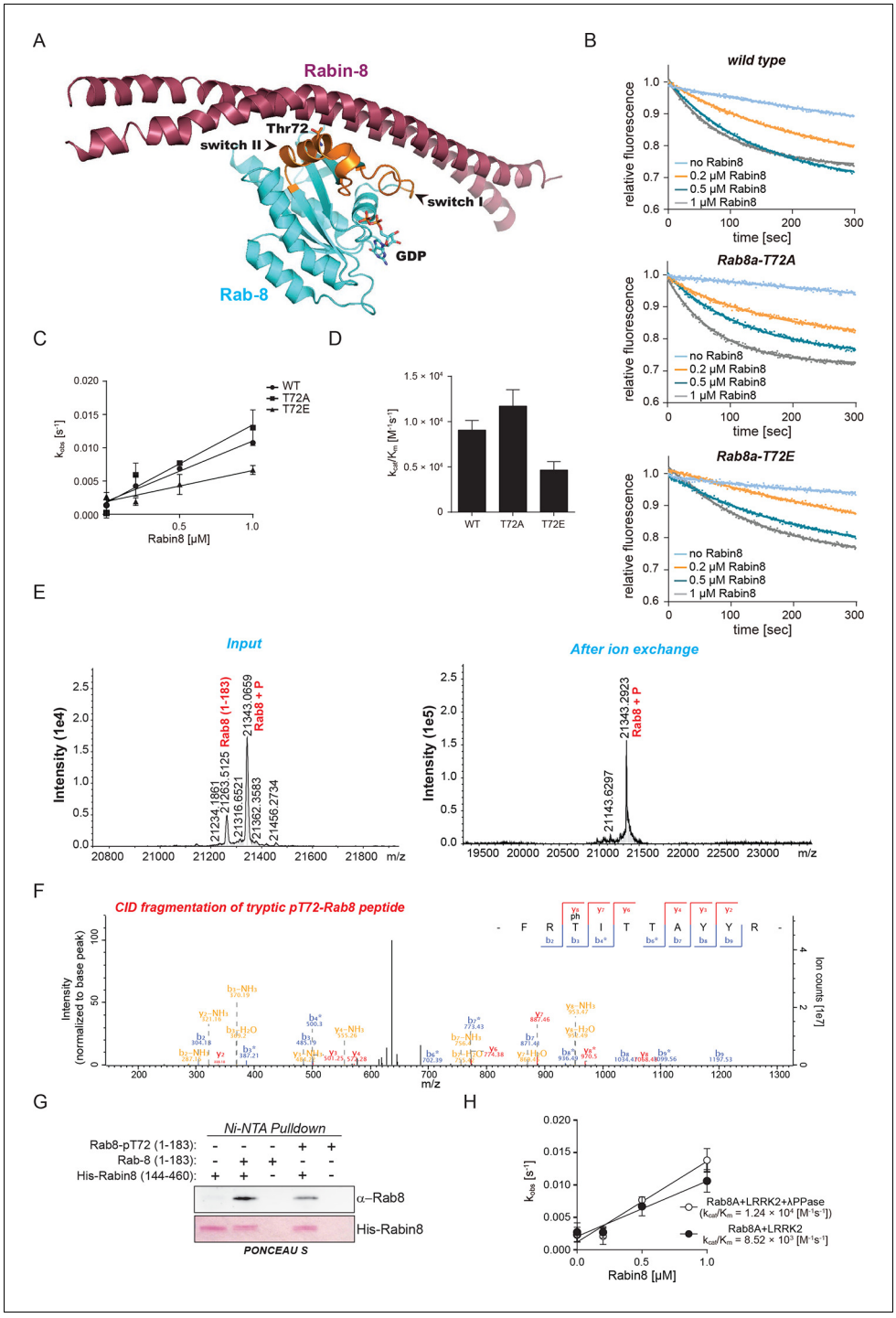

Figure 5—figure supplement 2. Rab8a guanine nucleotide exchange assays. (**A**) Ribbon structure of Rab8a in complex with Rabin8 (PDB: 4LHY). The LRRK2 phosphorylation site (T72) situated in the switch II region and forming close contact with Rabin8 is indicated. (**B**) Kinetics of mant-GDP dissociation from Rab8a (wt, T72A, and T72E) by Rabin8. (**C**) and (**D**) Representation of the observed rate constants (k_{obs}) and catalytic efficiencies (k_{cat}/K_m) for the same reactions. (**E**) ESI-TOF mass determination of Rab8a after in vitro phosphorylation by LRRK2-G2019S (left) and after enrichment of phosphorylated Rab8a by ion-exchange chromatography (right). (**F**) Collision-induced dissociation (CID) fragmentation spectrum of the tryptic pT72-Rab8a peptide, which was identified after phosphorylation of Rab8a by LRRK2 followed by enrichment of the phosphorylated form by ion exchange chromatography. (**G**) Ni^{2+}-NTA pull-down of Rab8a (non-phosphorylated or phosphorylated on T72) by HIS-

Figure 5—figure supplement 2 continued on next page

Figure 5—figure supplement 2 continued

tagged Rabin8 using purified components. (**H**) Representation of the observed rate constants (k_{obs}) and catalytic efficiencies (k_{cat}/K_m) for the indicated reactions. Error bars are mean ± SD (n=3).

DOI: 10.7554/eLife.12813.015

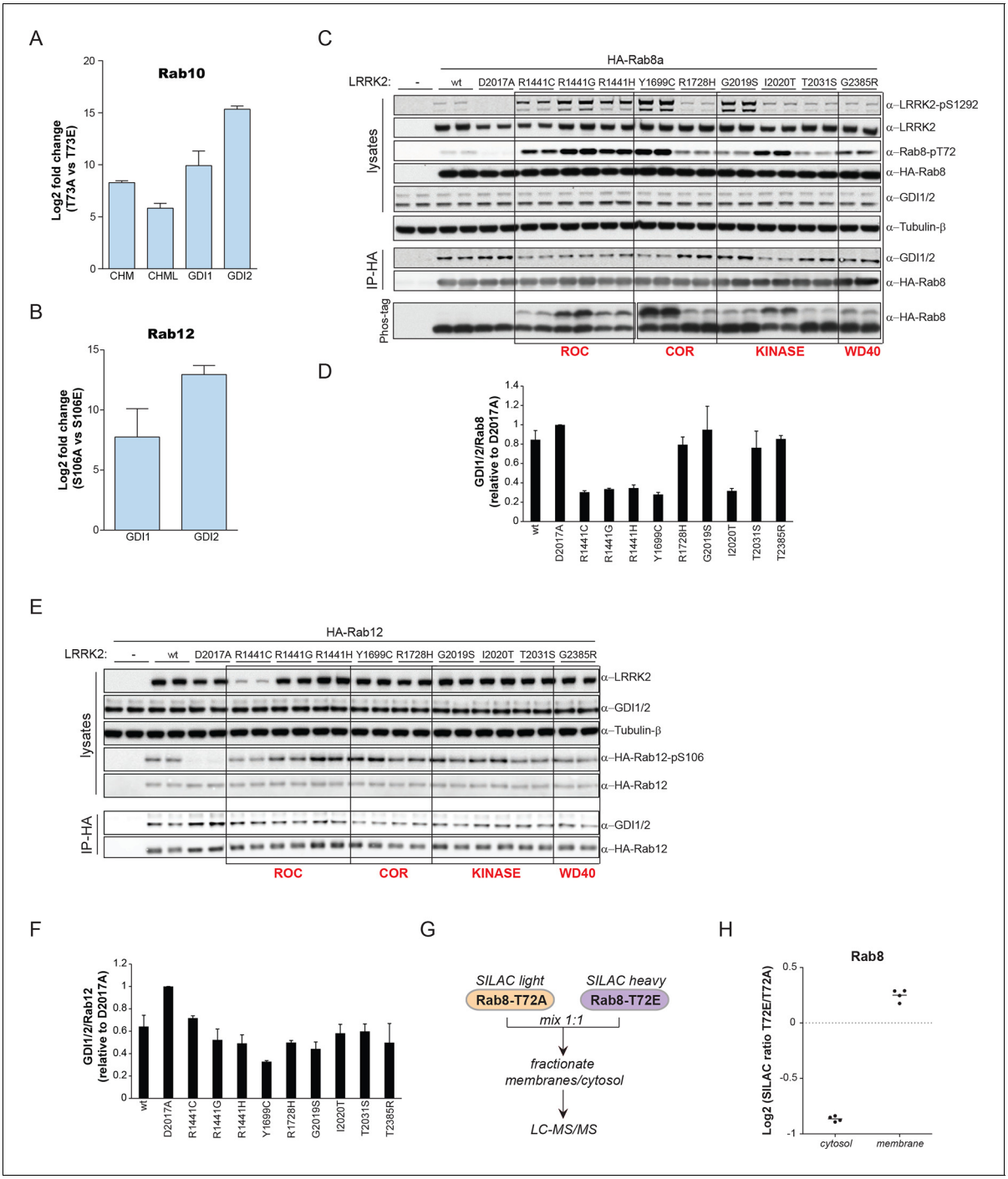

Figure 6. PD pathogenic LRRK2 mutations interfere with Rab-GDI1/2 association. (**A**) Fold changes (T73A/T73E, n=3) of indicated MS-quantified Rab10 interactors. (**B**) Same as (A) but S106A-Rab12 and S106E-Rab12 (n=4). (**C**) Different LRRK2 versions were co-expressed with Rab8a in HEK293 cells, lysates subjected to immunoblot analysis or immunoprecipitation using α-HA antibodies and indicated signals quantified (**D**). (**E**) and (**F**) Same as (**C**) with Rab12 expression. (**G**) Scheme for analyzing T72A-Rab8a and T72E-Rab8a subcellular protein distributions in a SILAC experiment. (**H**) SILAC ratios (Log2) of T72E-Rab8a/T72A-Rab8a proteins in the cytosolic and membrane fraction of HEK293 cells. PD, Parkinson's disease.

DOI: 10.7554/eLife.12813.016

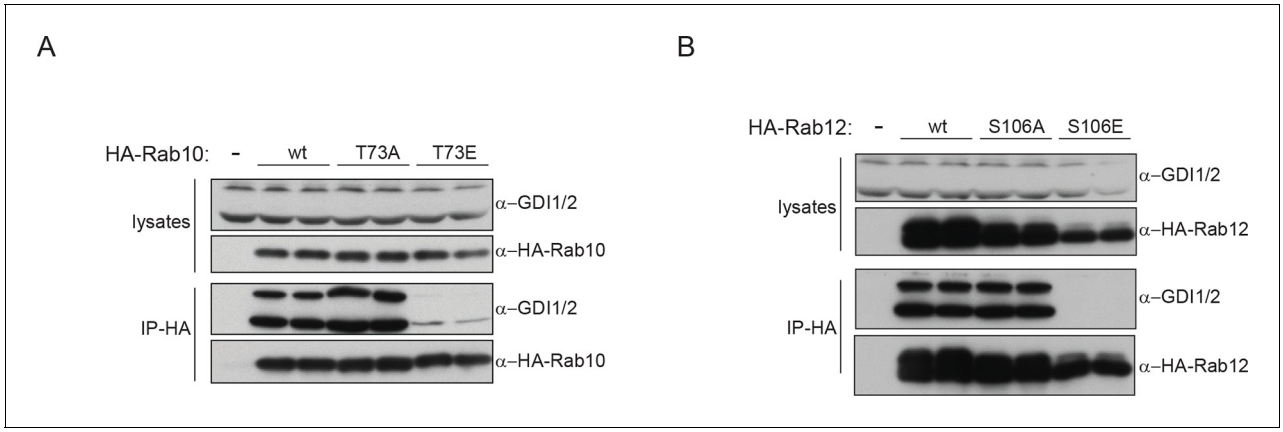

Figure 6—figure supplement 1. Rab10/12-GDI interactions. (**A**) HA-Rab10 constructs (wt, T73A, T73E) were expressed in HEK293 cells and lysates subjected to α-HA immunoprecipitation before western blotting. (**B**) Same as (**A**) using HA-Rab12 (wt, S106A, S106E). wt, wild type.
DOI: 10.7554/eLife.12813.017

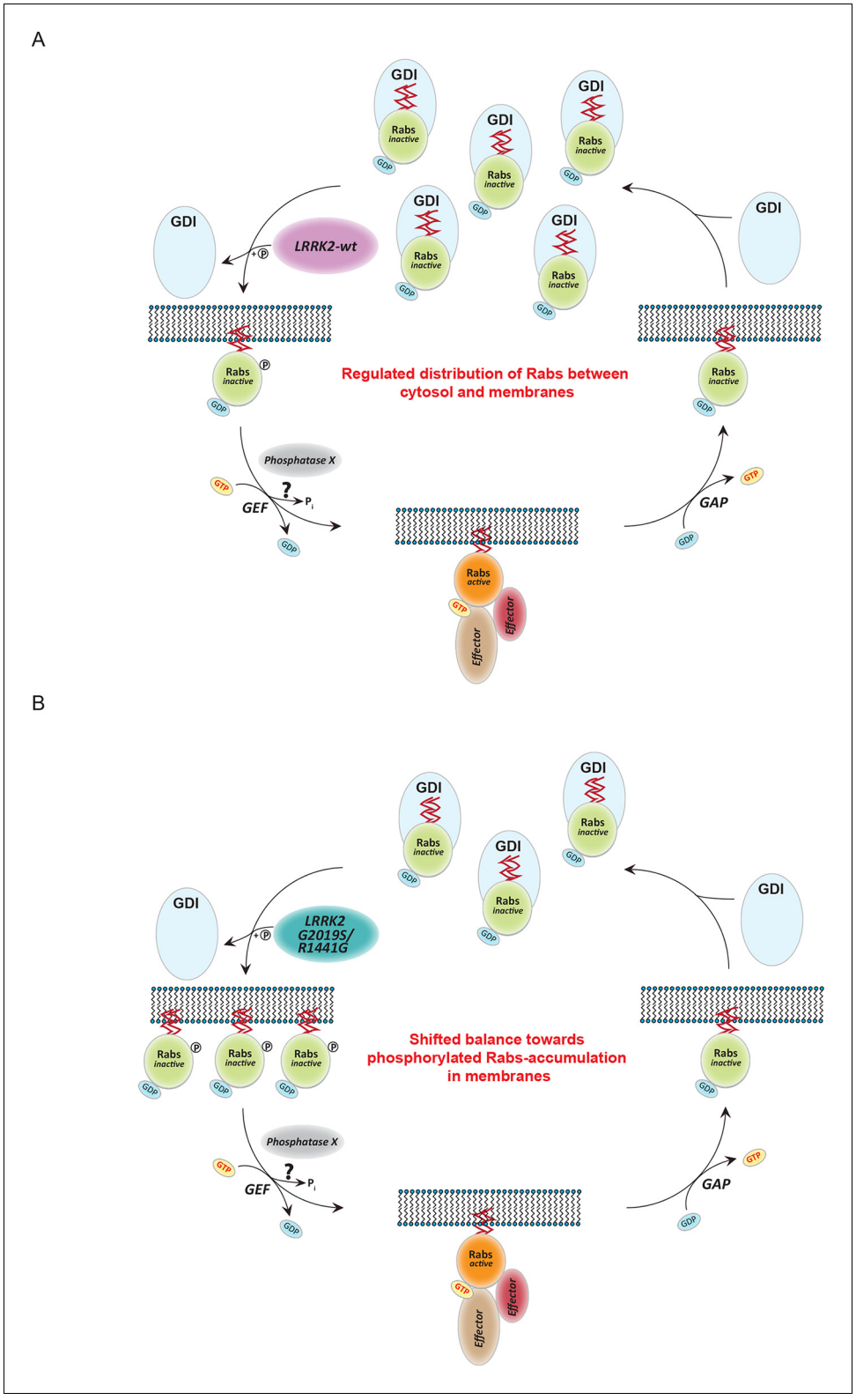

Figure 7. Model of Rab GTPase phosphorylation by LRRK2 and its outcome. (**A**) Rab GTPases (Rabs) cycle between an inactive (GDP-bound) and an active state (GTP-bound) between cytosol and membranes, respectively. Geranyl-geranyl-modified Rab GTPases in their GDP-bound state are tightly bound by guanine dissociation inhibitors (GDIs) in the cytosol. LRRK2 aids the insertion of Rabs in their specific target membrane. After removal of the LRRK2 phosphorylation site, guanine exchange factors (GEFs) facilitate exchange of GDP to GTP. This in

Figure 7 continued on next page

Figure 7 continued

turn allows binding to effector proteins and membrane trafficking events. Next, a Rab-specific GTPase-activating protein (GAP) assists in the hydrolysis of GTP followed by removal of the Rab GTPase from the target membrane by GDIs. (**B**) In pathogenic conditions, in which LRRK2 is hyperactive, RabGTPases have strongly diminished affinities for GDIs. As a result, the equilibrium between membrane-bound and cytosolic Rabs is disturbed, which may contribute to LRRK2 mutant carrier disease phenotypes. Model adapted and modified from (***Hutagalung and Novick, 2011***).

DOI: 10.7554/eLife.12813.018